

Photo-nuclear collisions in Pythia 8

I. Helenius and M. Utheim

University of Jyväskylä, Department of Physics, P.O. Box 35, FI-40014 University of Jyväskylä, Finland
Helsinki Institute of Physics, P.O. Box 64, FI-00014 University of Helsinki, Finland



We present a new extension in PYTHIA Monte Carlo event generator that allows to simulate the leading contribution in collisions of a real photon and a heavy ion. The model is based on a vector meson dominance (VMD) where a real photon is modelled as a linear combination of different vector-meson states, and an extension of ANGANTYR, the heavy-ion model in PYTHIA, that allow simulations of a generic hadron colliding with an ion target. We first verify the VMD implementation by comparing simulations to HERA photoproduction data. Then we present simulated results corresponding to event selection criteria applied in a recent ATLAS analysis for ultra-peripheral Pb-Pb collisions at the LHC. We find that the simulated results are in line with the ATLAS data when accounting for the limited detector efficiency for charged-particle reconstruction. We also consider two-particle correlations and study whether the simulated events reproduce the collective behaviour seen in the ATLAS γ -Pb data.

DOI: <https://doi.org/10.17161/9279nk67>

Keywords: Monte Carlo event generation, Ultra-peripheral collisions, photoproduction, charged-particle production, collectivity

1 Introduction

Ultraperipheral heavy ion collisions (UPCs)^{1,2} provide the first opportunity to study photo-nuclear interactions at collider energies. In addition to exclusive processes, the photon projectile emitted by the other beam nucleus may also break up the target nucleus in the interaction. Such collisions result as a complex hadronic final state. Monte Carlo event generators provide the necessary modelling to describe the collision process from the primary scattering to the long-lived hadrons measured in the detectors. The highly-virtual partons created in the hard scattering are evolved with DGLAP evolution equations to generate QCD radiation in the collinear approximation³ and after reaching non-perturbative scales, the partons form colour-neutral hadronic states that decay into stable ones. In case of hadronic collisions additional particle production takes place from multiparton interactions (MPIs) and beam remnants⁴.

In this work we present the necessary extensions to the PYTHIA Monte Carlo event generator⁵ that allows to simulate UPCs. We model the flux of photons from heavy nuclei using equivalent photon approximation (EPA)⁶. Unlike in the case of point-like leptons, the virtuality of photons emitted by charged hadrons and nuclei are limited and thus these can be assumed as real photons. Such photons can fluctuate into a hadronic state and simulations for these events will require all the same components as any other hadronic collision including beam remnants and MPIs. Furthermore, in case of nuclear target also subsequent collisions with multiple nucleons needs to be accounted for.

The main motivation for the present extensions is provided by the recent ATLAS analysis⁷ which studies the charged-particle production in UPCs at the LHC. An interesting observation in the analysis was the finite values for Fourier coefficients fitted to two-particle azimuthal correlations using a template fitting procedure. Such effects are typically connected to hydrodynamic flow in heavy-ion collisions. In this study we compare the simulated results to the measurement including multiplicity and pseudorapidity distributions and perform a similar template fitting to two-particle correlations. Such a setup is not only relevant for the UPCs at the LHC but similar γ -A processes can be studied also in future Electron-Ion Collider (EIC)⁸.

2 Theoretical background

2.1 Structure of a real photon

For hard-process generation that initiates the simulation chain we apply collinear factorization. In this framework the long-distance physics describing the structure of the incoming beams can be factorized from the short-distance interactions that can be calculated with perturbative QCD (pQCD). The structure of hadrons can be encoded into parton distribution functions (PDFs), $f_i^A(x_A, \mu^2)$, which describe the number distribution of parton i at the momentum fraction x_A inside a particle A when probed at scale μ^2 . In this framework the differential cross section to produce two partons, k and l , in a photo-initiated process can be computed from

$$d\sigma^{AB \rightarrow kl+X} = f_\gamma^B(x) \otimes f_j^\gamma(x_\gamma, \mu^2) \otimes f_i^A(x_A, \mu^2) \otimes d\sigma^{ij \rightarrow kl}, \quad (1)$$

where $f_\gamma^B(x)$ is the photon flux from beam particle B and x the momentum fraction of the photon wrt. the beam particle. The PDFs of the photon, $f_j^\gamma(x_\gamma, \mu^2)$ can be written as a sum of different components: direct, anomalous and hadron-like

$$f_i^\gamma(x_\gamma, \mu^2) = f_i^{\gamma, \text{dir}}(x_\gamma, \mu^2) + f_i^{\gamma, \text{anom}}(x_\gamma, \mu^2) + f_i^{\gamma, \text{hl}}(x_\gamma, \mu^2). \quad (2)$$

In case of direct contribution the incoming photon is simply the initiator of the hard process and we can replace $f_i^{\gamma, \text{dir}}(x_\gamma, \mu^2) = \delta_{i\gamma} \delta(1 - x_\gamma)$. For the anomalous component, where the photon splits into quark-antiquark pair perturbatively, the PDF can be directly calculated. For the hadron-like part the scale evolution can still be derived from DGLAP equations but a non-perturbative input is needed. This can either be fitted to data or it can be modelled with a vector-meson dominance (VMD) model where this state is given by a linear combination of vector-meson states⁹. In this study we will consider both approaches for the hadron-like part. Together with the anomalous part this form the resolved-photon contribution. In case of VMD the cross section for the collision between a hadron-like photon and a nucleon n is given by

$$\sigma^{\text{VMD}-n} = \sum_V \frac{4\pi\alpha_{\text{em}}}{f_V^2} \sigma^{V-n}, \quad (3)$$

where the couplings f_V can be obtained from data¹⁰.

When we apply the DGLAP-evolved PDFs for resolved photons with anomalous component, we need to include a term describing the $\gamma \rightarrow q\bar{q}$ splitting into the parton-shower algorithm. Such a term is included into the default parton shower in PYTHIA. Sampling such splitting during the evolution will collapse the photon back to an unresolved state where no MPIs or beam remnants are needed.

2.2 Photon fluxes

The photon fluxes for different beam configurations can be calculated from EPA. In case of electron-proton collisions the photon flux becomes

$$f_\gamma^e(x, Q^2) = \frac{\alpha_{\text{em}}}{2\pi} \frac{1}{Q^2} \frac{1 + (1-x)^2}{x}, \quad (4)$$

where the upper limit for the virtuality is obtained from the experimental setup and the lower limit follows from kinematical consideration giving $Q_{\text{min}}^2 \approx m_e^2 x^2 / (1-x)$. Having the flux differential also in Q^2 allows for sampling of the virtuality and deriving complete kinematics of the event, including transverse momentum of the outgoing lepton and the intermediate photon. Also photon flux from protons has been implemented in Pythia where a form factor has to be included in the calculation to account for the finite size of the emitting particle and to keep it intact.

In case of heavy ions it is more convenient to work out the flux in impact-parameter space as this allows for a straightforward rejection of events where the beam particles would interact hadronically via short-range strong interaction. Assuming a point-like flux and a sharp cut-off for the allowed impact parameter values we have

$$f_\gamma^A(x) = \frac{2\alpha_{\text{em}} Z^2}{x\pi} \left[\xi K_1(\xi) K_0(\xi) - \frac{\xi^2}{2} (K_1^2(\xi) - K_0^2(\xi)) \right], \quad (5)$$

where $\xi = b_{\text{min}} x m$, m is the per-nucleon mass for nucleus A and K_i modified Bessel functions of the first kind. We select $b_{\text{min}} = 2R_A$, where R_A is the radius of the colliding nuclei to reject the nuclear

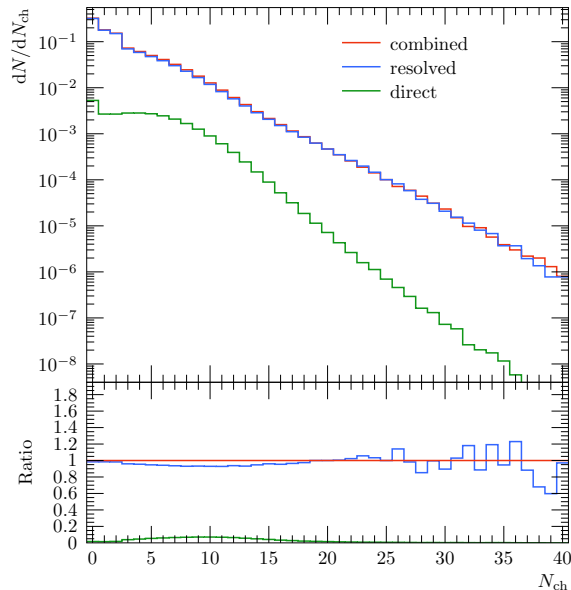


Figure 1 – Multiplicity distribution in photoproduction in electron-proton collisions corresponding to event selection criteria in the ZEUS analysis from complete simulations (red) and from resolved (blue) and direct (green) components separately.

overlap. This approximation works well in the kinematic region relevant for this study but break down for final states which require a large energy for the intermediate photons¹¹. In addition to hadronic break-up probability factor it has been shown that to match the experimental event selection criteria also a rejection for subsequent electro-magnetic interactions could be significant¹².

3 Photoproduction in electron-proton collisions

Due to the low virtuality of photons emitted by charged hadrons and heavy ions, the UPC events are similar to photoproduction that has been extensively studied with proton target in HERA collider. We can therefore use these data to validate our implementation of photon structure and compare the VMD approach to the full description of quasi-real photons. Here we will apply a recent ZEUS analysis¹³ which focuses on high-multiplicity events where the resolved photons are expected to dominate the cross section. As a validation for the previous statement we show the multiplicity distribution of charged particles from our simulations in figure 1. In addition to the total multiplicity also the direct and resolved contributions are shown separately. The direct contribution is at most 10% for events with around 10 charged particles. Furthermore, in the region where $N_{\text{ch}} > 20$, direct photons contribution well below 1% and can be safely neglected in the following studies. We note that the definition of N_{ch} does not include all particles in the event but matches the acceptance and particle-selection criteria applied in the ZEUS analysis.

We present comparisons with the simulated results and the data in figure 2 for charged-particle multiplicity, N_{ch} , and pseudorapidity, η distribution. In case of simulation, we show results using the full photoproduction setup as implemented in PYTHIA (gm-p) and by using only the VMD model (vmd-p). Furthermore, we vary the parameter $p_{\text{T},0}^{\text{ref}}$, that controls the probability for MPIs, for both setups within values $p_{\text{T},0}^{\text{ref}} = 3, 4$ GeV. In case of N_{ch} distribution we notice that the probability of large multiplicity events are sensitive to the parameter value applied for $p_{\text{T},0}^{\text{ref}}$. Especially in case of full photoproduction implementation we find a factor of five difference between the two applied values at the highest multiplicities. With the VMD-only calculation, with the two parameter values lead somewhat reduced variation. More importantly we notice that the two applied approaches are in a good agreement with each other and the data and that these data could provide further constraints for MPI modelling in photon-hadron collisions. For the η distribution we again notice that the calculated results from both models are in a good agreement with each other and the experimental data. As a large fraction of events passing the selection criteria are from the low end of multiplicity distribution, the sensitivity to $p_{\text{T},0}^{\text{ref}}$ parameter is significantly reduced compared to N_{ch} distribution. We can thus conclude that, while there are some underlying theoretical uncertainty, both applied approaches, the full photoproduction model with the resolved-photon

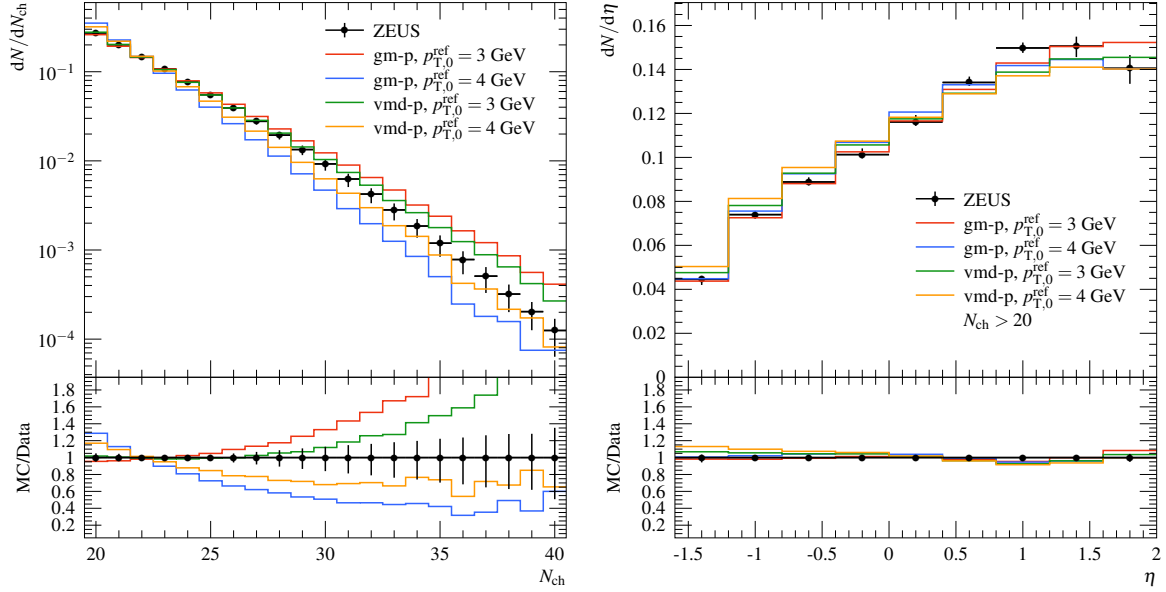


Figure 2 – Charged-particle multiplicity and rapidity distributions in photoproduction in electron-proton collisions from a ZEUS analysis compared with the simulations from full photoproduction (gm-p) model and VMD-based implementation (vmd-p) for resolved photons with two different values for parameter $p_{T,0}^{\text{ref}}$.

PDFs and the VMD-based model, are adequate to describe the minimum bias photon-proton collisions especially in case of the high-multiplicity events.

4 Ultraperipheral collisions at the LHC

4.1 Photon-ion collisions

As a first step for full model for interactions between a real photon and a heavy nucleus in ultraperipheral heavy-ion collisions we have extended recent work that enable generation of collisions with generic hadron beams with varying energy on a proton target¹⁴ in PYTHIA 8 to handle also collisions with a nuclear target. The nuclear effects are modelled with the existing Angantyr model¹⁵ where the heavy ion collisions are generated by deriving the nucleon-nucleon collisions from a Monte Carlo Glauber model. The interaction probabilities include cross section fluctuations and sampling for the type of the primary interaction which can be non-diffractive, single diffractive, double diffractive or elastic. The secondary interactions are modelled using diffractive excitations which account for the reduced energy which the projectile particle has lost in the primary interaction. The Angantyr model builds up the nuclear collisions from a collection of nucleon-nucleon events generated with Pythia, which we have extended to handle also a generic hadron as a beam particle. In particular the cross section fluctuations in the Angantyr model has been adjusted to handle also such beam configurations.

Comparison between different projectiles for the charged-particle multiplicity and rapidity distributions in a hadron-lead nucleus collision at $\sqrt{s_{\text{nn}}} = 5.02$ TeV are shown in figure 3. The considered projectile particles include proton as a baseline and ρ , ϕ and J/Ψ to demonstrate the components of the VMD model. The multiplicity distribution has two distinct components, a peak at low multiplicity which arises from diffractive and elastic events and an another peak around 150-350 particles from non-diffractive events. The multiplicity distribution from the non-diffractive events becomes more narrow when switching the projectile from protons to vector mesons. This is due to having less secondary collisions in case of vector mesons due to lower non-diffractive cross section that determines the effective size of the projectile in the Glauber model. In the rapidity distribution we notice that the distribution of generated particles are more symmetric in case of collisions with vector-meson projectiles. This mainly follows from the same reason as above since the particles produced in the primary interactions are symmetric in rapidity and the asymmetry is mainly generated by the secondary interactions that are less frequent in case of vector mesons. Also the shape of the PDFs play some role here especially in case of J/Ψ where the heavy valence quarks carry a large fraction of the momenta of the particle that results as an almost symmetric

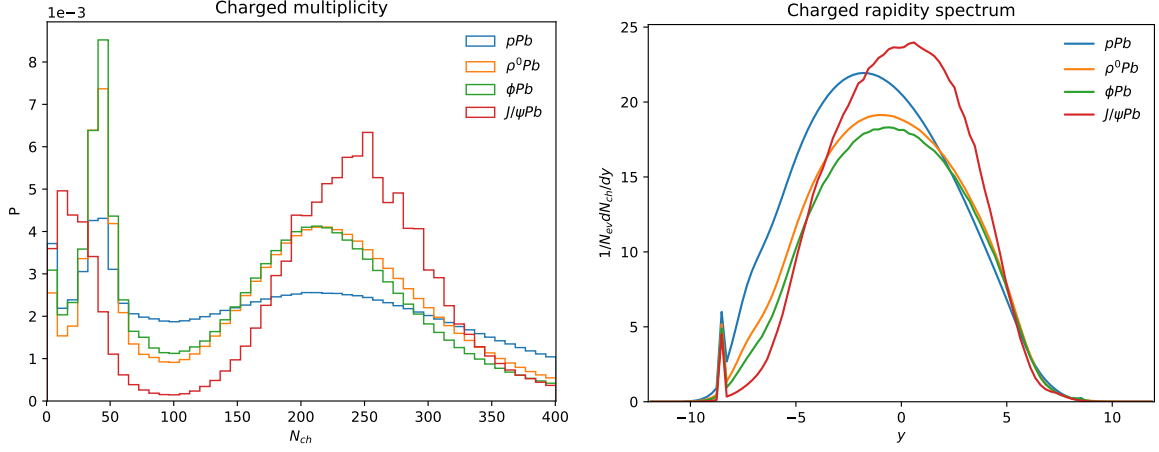


Figure 3 – Multiplicity (left) and rapidity (right) distributions of different hadron-nucleus collisions at $\sqrt{s_{NN}} = 5.0$ TeV with lead target and proton (blue), ρ^0 (orange), ϕ (green) and $J\Psi$ (red) projectiles.

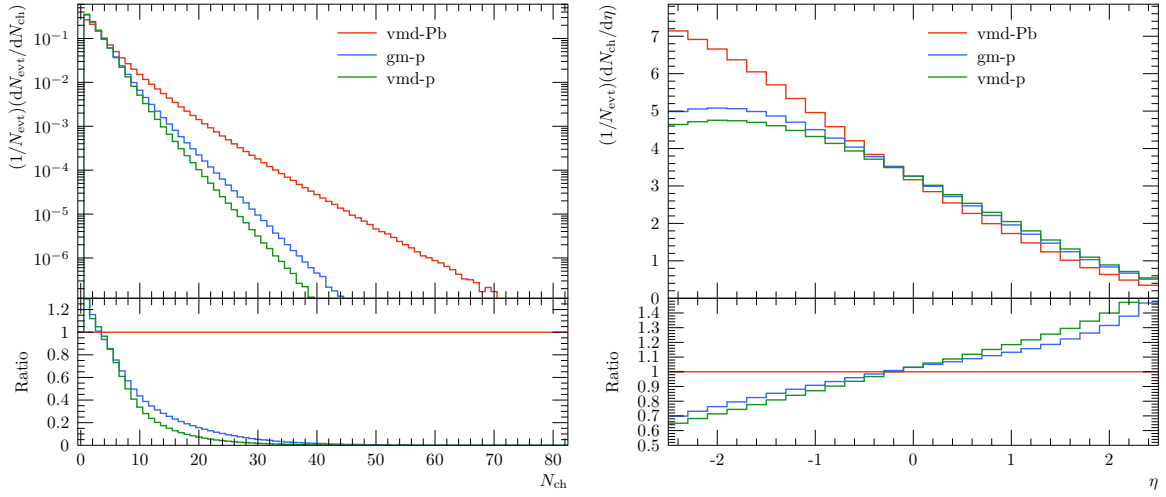


Figure 4 – Multiplicity (left) and rapidity (right) distributions for VMD-Pb simulations (red) compared to simulations with proton target applying VMD model (green) and full photoproduction (blue) at $\sqrt{s_{NN}} = 5.02$ TeV.

rapidity distribution even with a nuclear target.

To account for the varying collisions energy from photon-flux sampling, the model parameters are fitted at a few fixed values in the specified energy range and then interpolated to obtain the values corresponding to the collision energy sampled according to the photon flux. Enabling this allows simulations for UPC events at the LHC with the VMD-nucleus setup based on the extended Angatyr model. We can compare these results then to the ATLAS data⁷ for different observables. The main caveat with this data is, however, that the relevant distributions for charged-particle multiplicity and rapidity distributions with a multiplicity cut have not been corrected for limited particle-detection efficiency and therefore are not available for direct comparisons. Thus we only show results of our simulations with VMD model using proton and nucleus targets and compare these with the full photoproduction with proton target that was included in ATLAS results. This allows to estimate the agreement with the data by comparing the relative difference between this baseline simulation and the VMD-Pb setup to the experimental one. Again, we consider charged-particle multiplicity and pseudorapidity distributions in figure 4. We apply the same event-selection criteria as in the ATLAS study including a cut for the sum-of-rapidity-gaps measure $\Sigma_\gamma \Delta\phi$. We also adjust the multiplicity cut applied for the η distribution with an efficiency correction estimated by comparing the N_{ch} from the gm-p setup in figure 4 to the one presented the ATLAS study giving an efficiency of 80% which is in line with previous ATLAS studies in different beam configurations⁶. With this corrections in place, we find that the simulated distributions are well in line with the experimental data.

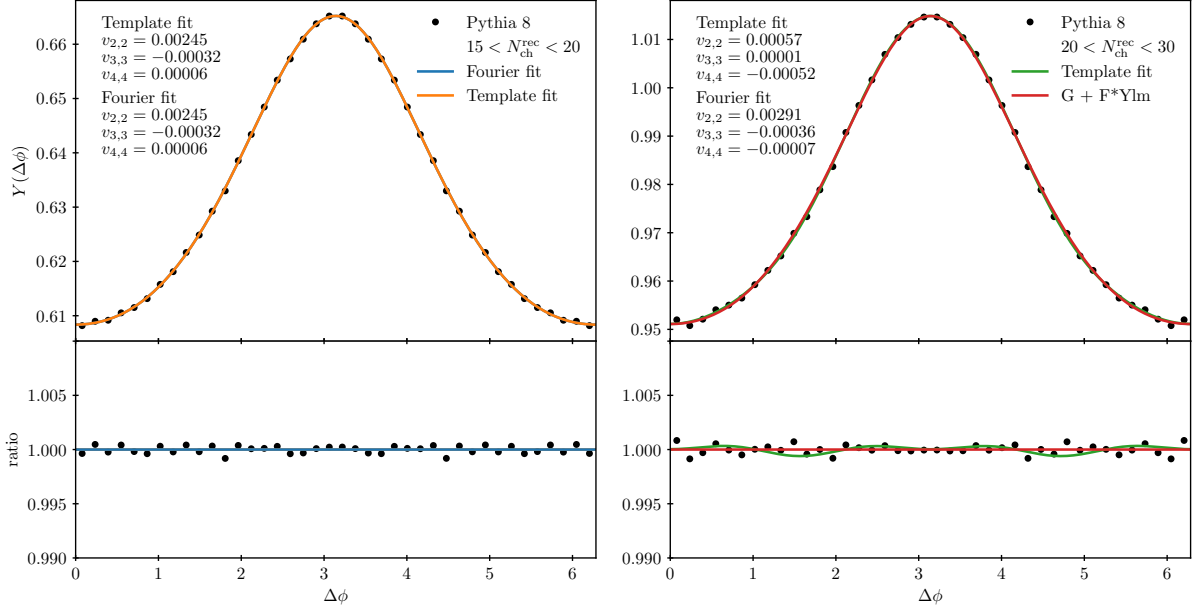


Figure 5 – An example of the template fitting procedure to the simulated data.

4.2 Correlations

Having a framework to successfully describe the single-particle properties in high-multiplicity γ -Pb events, we can study such collisions with multiparton correlations. A particularly interesting observation in the ATLAS study was the observation of finite values for v_2 and v_3 that are typically considered as a signature of collective behaviour. While the template fitting procedure applied in the ATLAS analysis should remove the “non-flow” contribution such as jet-like correlations, it is still interesting to check whether any similar effects would arise from the MC simulations without any explicit final-state effects. The reason for this is that the binning to low- and high-multiplicity events will also bias the underlying energy distributions since higher collision energy for the γ -Pb system will lead to higher average event multiplicity. Therefore the low-multiplicity event sample needed for the template fit might not capture all the jet-like correlations present in the high-multiplicity events at higher collision energy.

The template fitting procedure involves a simultaneous fit of two-particle correlation function $Y(\Delta\phi)$ for low- (LM) and high-multiplicity (HM) event samples which are obtained by integrating over relative pseudorapidity separation, $\Delta\eta$, with limits $2.0 < |\Delta\eta| < 5.0$ to focus on long-range η correlations. In case of low-multiplicity events, the following truncated Fourier series is applied

$$Y^{\text{LM}}(\Delta\phi) = c_0 + 2 \cdot \sum_{n=1}^4 c_n \cos(n\Delta\phi), \quad (6)$$

where c_n are free parameters that can be related to flow harmonics v_n . In case of HM event sample the $Y(\Delta\phi)$ is fitted with

$$Y^{\text{HM}}(\Delta\phi) = F \cdot Y^{\text{LM}}(\Delta\phi) + G \left[1 + 2 \cdot \sum_{n=2}^4 v_{n,n} \cos(n\Delta\phi) \right], \quad (7)$$

where now a scaled $Y^{\text{LM}}(\Delta\phi)$ is used as a baseline and $v_{n,n}$ allow for additional modulation for the HM sample. The scaling factors F and G are connected so in total there are 8 free parameters in the fit. An example of the fitting procedure is shown in figure 5 where $Y^{\text{LM}}(\Delta\phi)$ and $Y^{\text{HM}}(\Delta\phi)$ are fitted to the simulated data simultaneously. We have also performed independent Fourier fits with 4 parameters corresponding to equation (6) to both LM and HM samples. In case of the former event class this allows to check that the full template fitting does not bias the LM sample fitting and in case of latter this provide the Fourier harmonics without the “non-flow” subtraction for comparison. For the example configuration in figure 5 we have taken $15 < N_{\text{ch}}^{\text{rec}} < 20$ for the LM sample and $20 < N_{\text{ch}}^{\text{rec}} < 30$ for the HM sample. Both particles, the trigger and the associated, had a transverse momentum of $0.4 < p_{\text{T}} < 2.0$ GeV.

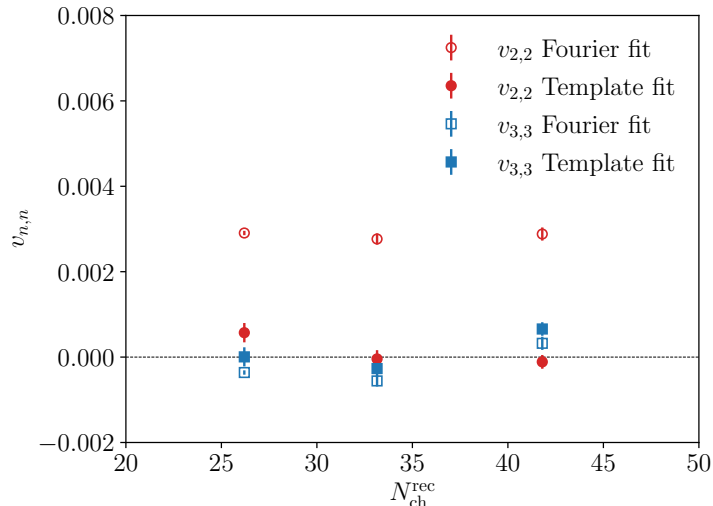


Figure 6 – Fitted values for $v_{2,2}$ (red) and $v_{3,3}$ (blue) from a direct Fourier fit, equation (6), (open markers) and a full template fit, equation (7), (closed markers) as a function of charged-particle multiplicity. Error bars quantify the fit uncertainty due to finite simulation statistics.

Similarly as in the ATLAS analysis, we have performed the fit with varying HM selection and plot the resulting $v_{n,n}$ values in figure 6. We notice that while the resulting values for $v_{2,2}$ and $v_{3,3}$ in case of a direct Fourier fit are in line with the measured ones, the values from a full template fit are consistent with zero in all considered multiplicity bins. This implies that our simulations do not reproduce the observed finite values of $v_{n,n}$ seen in the ATLAS γ -Pb data when the template fitting is applied. This confirms that the positive values for v_n in the ATLAS analysis are a result from a final-state (or initial-state) collectivity and not due to biased collision energy due to multiplicity sampling and that the template method work as expected also when applied to data with multiplicity binning in γ -Pb.

5 Summary and Outlook

We have presented a new model to simulate collisions between real photons and heavy ions based on a vector-meson dominance model within PYTHIA Monte Carlo event generator. In this model the photon is described as a linear combination of different vector-mesons states, ρ , ω , ϕ and J/Ψ . While this model does only account for the hadron-like part of the photon structure, such events are expected to dominate the total cross section and especially the high-multiplicity events. Unlike the direct-photon component, these resolved photons may interact with other nucleons inside a nucleus and give rise to events with large multiplicity. We have demonstrated that this contribution is indeed the dominant one in high multiplicity events and that the model is in line with the multiplicity distributions measured at HERA for γ -p collisions. Furthermore, we notice that when accounting for the limited efficiency, the model provides a good description of the charged-particle multiplicity and rapidity distributions in γ -Pb measured by ATLAS in ultra-peripheral Pb-Pb collisions.

We have also considered two-particle correlations and derived Fourier coefficients from the simulated events using a similar template fitting procedure as in the ATLAS analysis. Here the low- and high-multiplicity event samples are simultaneously fitted with truncated Fourier series which is supposed to remove possible “non-flow” jet-like contributions. While it is non-trivial that this procedure should work also in case of varying photon-energy spectrum which can lead to biased collision energy distribution when multiplicity binning is applied, we find that the resulting $v_{n,n}$ coefficients are consistent with zero. Thus we conclude that the observed collectivity in γ -Pb events is not reproduced with the default PYTHIA hadronization model. There have been recent studies, however, where including string interactions, such rope hadronization and string shoving, in the hadronization model have given rise to similar collective effects when applied to high-multiplicity proton-proton and proton-lead collisions. We plan to study these effects in case of γ -Pb in a future study. Also, the presented framework will serve as a starting for a more complete simulations of photon-ion collisions relevant also for the EIC.

Acknowledgments

We acknowledge the financial support from the Research Council of Finland, Project No. 331545. The work has been supported also through the Centre of Excellence in Quark Matter funded by the Research Council of Finland. The reported work is associated with the European Research Council project ERC-2018-ADG-835105 YoctoLHC. We acknowledge grants of computer capacity from the Finnish Grid and Cloud Infrastructure (persistent identifier `urn:nbn:fi:research-infras-2016072533`).

References

1. C. A. Bertulani, S. R. Klein and J. Nystrand, *Ann. Rev. Nucl. Part. Sci.* **55** (2005), 271-310 doi:10.1146/annurev.nucl.55.090704.151526 [arXiv:nucl-ex/0502005 [nucl-ex]].
2. S. Klein and P. Steinberg, *Ann. Rev. Nucl. Part. Sci.* **70** (2020), 323-354 doi:10.1146/annurev-nucl-030320-033923 [arXiv:2005.01872 [nucl-ex]].
3. T. Sjöstrand and P. Z. Skands, *Eur. Phys. J. C* **39** (2005), 129-154 doi:10.1140/epjc/s2004-02084-y [arXiv:hep-ph/0408302 [hep-ph]].
4. T. Sjöstrand and P. Z. Skands, *JHEP* **03** (2004), 053 doi:10.1088/1126-6708/2004/03/053 [arXiv:hep-ph/0402078 [hep-ph]].
5. C. Bierlich, S. Chakraborty, N. Desai, L. Gellersen, I. Helenius, P. Ilten, L. Lönnblad, S. Mrenna, S. Prestel and C. T. Preuss, *et al. SciPost Phys. Codeb.* **2022** (2022), 8 doi:10.21468/SciPostPhysCodeb.8 [arXiv:2203.11601 [hep-ph]].
6. V. M. Budnev, I. F. Ginzburg, G. V. Meledin and V. G. Serbo, *Phys. Rept.* **15** (1975), 181-281 doi:10.1016/0370-1573(75)90009-5
7. G. Aad *et al.* [ATLAS collaboration], *Phys. Rev. C* **104** (2021) no.1, 014903 doi:10.1103/PhysRevC.104.014903 [arXiv:2101.10771 [nucl-ex]].
8. R. Abdul Khalek, A. Accardi, J. Adam, D. Adamiak, W. Akers, M. Albaladejo, A. Al-bataineh, M. G. Alexeev, F. Ameli and P. Antonioli, *et al. Nucl. Phys. A* **1026** (2022), 122447 doi:10.1016/j.nuclphysa.2022.122447 [arXiv:2103.05419 [physics.ins-det]].
9. M. Gluck, E. Reya and A. Vogt, *Phys. Rev. D* **46** (1992), 1973-1979 doi:10.1103/PhysRevD.46.1973
10. T. H. Bauer, R. D. Spital, D. R. Yennie and F. M. Pipkin, *Rev. Mod. Phys.* **50** (1978), 261 [erratum: *Rev. Mod. Phys.* **51** (1979) no.2, 407] doi:10.1103/RevModPhys.50.261
11. K. J. Eskola, V. Guzey, I. Helenius, P. Paakkinen and H. Paukkunen, [arXiv:2404.09731 [hep-ph]].
12. [ATLAS collaboration], ATLAS-CONF-2022-021.
13. I. Abt *et al.* [ZEUS collaboration], *JHEP* **12** (2021), 102 doi:10.1007/JHEP12(2021)102 [arXiv:2106.12377 [hep-ex]].
14. T. Sjöstrand and M. Uthmeim, *Eur. Phys. J. C* **82** (2022) no.1, 21 doi:10.1140/epjc/s10052-021-09953-5 [arXiv:2108.03481 [hep-ph]].
15. C. Bierlich, G. Gustafson, L. Lönnblad and H. Shah, *JHEP* **10** (2018), 134 doi:10.1007/JHEP10(2018)134 [arXiv:1806.10820 [hep-ph]].
16. M. Aaboud *et al.* [ATLAS collaboration], *Phys. Rev. C* **96** (2017) no.2, 024908 doi:10.1103/PhysRevC.96.024908 [arXiv:1609.06213 [nucl-ex]].